HEAT AND MASS TRANSFER
AND PHYSICAL GASDYNAMICS

Experimental Study of the Influence of the Shape of the Gap between the Rib and Flat Plate on the Near-Wall Flow Structure and Heat Transfer

S. A. Isaev[a], V. N. Afanasiev[b], K. S. Egorov[b], and Dehai Kong[b], *

[a]St. Petersburg State University of Civil Aviation, St. Petersburg, 196210 Russia
[b]Bauman Moscow State Technical University, Moscow, 105005 Russia
***e-mail: kongdehai2013@gmail.com**

Abstract—The article presents an analysis of the results of an experimental study of the dynamic and thermal characteristics of the turbulent boundary layer of the air near a heated plate at q_w = const with rectangular ribs having slit channels of different geometry: confusor, diffuser, and plane-parallel. The slit channel is located between the plate and the lower rib wall. The results are compared with similar data for a solid rib without the slit channel. A Pitot–Prandtl microprobe with a microthermocouple and the Dantec Dynamics hot-wire anemometer were used, thus making it possible to study the laminar sublayer, the transition domain, and the outer part of the boundary layer. The influence of the slit profile on the average and the pulsation characteristics of the turbulent dynamic and thermal boundary layers in the median section of the plate with the slit rib is revealed. It is found that the separated zone disappears in the flow behind the ribs with the confusor slit.

INTRODUCTION

The design and creation of highly efficient, compact, and reliable cooling systems are an urgent problem, one that is often successfully solved with the application of efficient methods of heat-transfer intensification. Methods that proposing to affect the flow, primarily on the boundary layer, with the use of different intensifiers, such as trenches [1, 2], ordered packages of spherical dimples [3, 4], various geometry fins, ribs, dimples [5−29], etc., are of great practical interest.

Experimental and theoretical studies of the flow structure in the flow around various kinds of ribs and dimples on the initially smooth surfaces are of significant practical interest, since the dimples and cavities (of construction or accidental origin) exist on many convective surfaces, e.g., in cases of spacecraft entering the atmosphere and undergoing micrometeorite blows and aerodynamic heating; turbine channels; empennage surfaces, etc. In the flow around ribs and the dimples, the boundary layer separation and its reattachment results in the occurrence of phenomena exerting a significant influence on the resistance and heat transfer. Many papers [10−17] focus on the comparison of the integral characteristics of the heat and impulse transfer; however, there are recently published works in which great attention is paid to the detailed study of the flow structure and the local characteristics of the flow and heat transfer near the heat-transfer intensifiers with the use of modern experimental and numerical diagnostics methods. Let us note the numerical study of flow and heat-transfer structure via direct numerical simulation (DNS) [18] and experimental studies involving particle image velocimetry (PIV) [19, 20].

One goal of the intensification of convective heat transfer is to affect the boundary layer by thinning or partly destroying it. The flow turbulization is connected with energy consumption; thus, in the development of efficient methods of heat-transfer intensification, rational selection of the turbulizator location and design appears to be of importance. In the most efficient intensification method, the impact is related to the wall liquid layers at a distance of about $y^+ \leq 30−100$ from the wall and does not influence the flow core [5, 6, 10, 30]. This very method will result in a significant increase in the heat-transfer coefficient upon a moderate increase in the friction coefficient, i.e., it increases advanced heat transfer as against the frictional drag. The ribs that sink into the boundary layer and somewhat enter (in height) the transition zone are of traditional interest: they insufficiently influence the profile resistance of the surface with the rib.

The organization of separation zones and vortical structures [31] is an efficient method of controlled impact on the near-wall turbulent flow. Transverse ribs or riffles located on the heat-transfer surface are one of the most popular means of vortex generation. Ribs and dimples can have different shape and sizes; these parameters significantly influence the boundary
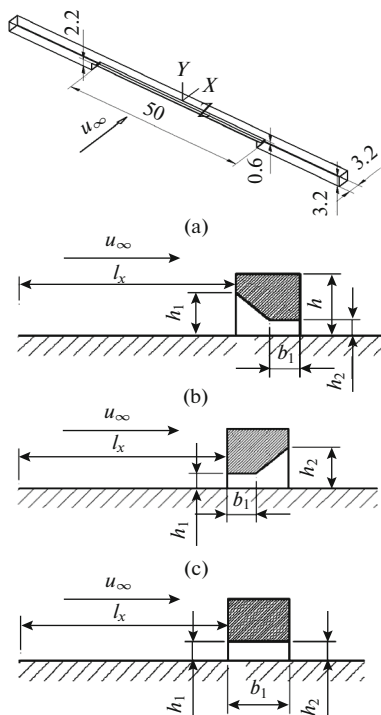
Fig. 1. Layout of the location of a rectangular slit rib on a plate: (a) with a confusor slit, (b) with a diffuser slit, (c) with a constant cross-section slit.

layer structure and the processes of heat and impulse transfer. The majority of available works (e.g., [10]) study the characteristics of separation flows and heat transfer in the channels with respect to the relative geometric sizes of the ribs. However, there are few studies of the external flow over surfaces with the ribs at different widths of the boundary layers. Analyses of the influence of the ratio of the rib height to the boundary layer thickness, of the space between the ribs to the rib height, of the rib width to the boundary layer thickness, the influence of the rib shape, its location at the different angles to the main flow, etc., are of interest. Note that, as a rule, relatively large ribs and ribs comparable to or exceeding the boundary layer thickness are studied [8, 9, 12–14]. The hydrodynamics and heat-transfer characteristics of the separation flow with variation in the blockage shape and height, including a reversed, backward-facing step and transverse thin rib (fin), were experimentally analyzed with a miniature Pitot–Prandtl tube and microthermocouples [12]. Soot-oil visualization was also used to determine the dimensions of the recirculation domain behind the backward-facing step and rib. As a rule, analysis of the works on heat transfer in the separation zones indicates a disturbance of the Reynolds' analogy in the separation domain, which is not in favor of heat transfer.

It is known that, with flow around a solid rib, low-velocity separation zones occur in front of it and behind it, thus significantly reducing the heat-transfer

coefficient in its vicinity. It was shown [21] that reduction or deletion of these zones can be achieved via rib perforation by slit-like channels. Such a slit-perforated rib can eliminate the separation zones due to the throttling effect [32]. It is known that the placement of permeable ribs on the channel wall increases heat-transfer efficiency as compared to a channel with solid ribs. The turbulent characteristics of the friction and heat transfer in a rectangular channel with pored ribs placed on one wall were studied experimentally [22]. They did not observe any zones with a low heat-transfer coefficient within the domain behind the pored ribs. The mechanisms of the impulse and energy transfer mechanisms with flow around a rib with a slit were studied in greater detail [23]. The flow structure with flow around permeable ribs were studied via PIV and surface visualization of the flow [20]. In addition, many experimental [24–26] and numerical [27–29] works pay special attention to the study of the characteristics of flow around detached ribs or fins. Detached and perforated ribs in a rectangular channel were experimentally analyzed [26]. All of the works deal predominantly with square or rectangular obstacles.

In the present work, we propose to intensify heat transfer via the application of rectangular, prolonged, slit, transverse ribs on a plate with the three kinds of slit profiles between the plate and the rib: a confusor slit, a diffuser slit, and a slit with a constant section. The presence of a gap between the rib and the channel wall forms the near-wall jet in a separate flow domain behind the rib.

EXPERIMENTAL

We conducted the studies in a subsonic, low-turbulent ($\varepsilon = 0.2\%$), open-type, aerodynamic tube that operates on the principle of suction. A detailed description of the experiment technique and facility is presented in [1, 3, 33]. We study (experimentally) the flow around a slit and rectangular and square ribs with a height of about $y^+ < 100$ where $y^+ = yu_\tau/\nu$.

We placed a rectangular rib with confusor, diffuser, and constant section slits with a height of $h = 3.2$ mm and a thickness of $b = 3.2$ mm on a heated flat wall perpendicular to the flow at a distance of $l_x = 460$ mm from the entrance into the working section. Figure 1 and Table 1 show the rib location, shape, and size. We maintained a velocity of the outer flow in the first section (at a distance of 425 mm from the entrance into the working part of the channel) of about 15.5 m/s. This corresponds to a Reynolds number (calculated according to the momentum thickness in that section) of Re** = 1500.

All measurements were made with a Pitot–Prandtl microprobe with a microthermocouple having a diameter of $d = 0.1$ mm; the probe was specially developed and created in order to operate in the boundary layer. The Dantec Dynamics hot-wire anemometer was also used. This made it possible to study the laminar sub-

layer, the transit domain of the boundary layer, and to obtain the average and pulsation characteristics of the flow. The longitudinal velocity profiles and its pulsations were measured in different sections of the boundary layer with a 55P11-type unifilar sensor with a Dantec Dynamics 90C10 module, a constant-temperature hot-wire anemometer (CTA). A 5-μm tungsten filament, 1.25 mm in length, was the sensing element. The temperature was measured with a Dantec Dynamics 90C20 temperature module, a constant-current hot-wire anemometer (CCA) that includes a miniature sensor with a 55P04-type gilded tungsten filament, 5 μm in diameter and 3 mm in total length, operating as the resistance thermometer. A coordinate system including the traverse probe, stepper motor, and power supply was used to sound the boundary layer. The accuracy of the movement detection by the coordinate device is about 0.02 mm. The hot-wire anemometer sensors were calibrated with a special calibrator. The ultimate relative error of velocity measurement with a MKV-250 micromanometer is within 1.2%. During the experiment, the amplitude of the signal for the actual instant velocity and temperature values was measured with a National Instruments 12-bit PCI-6040E data acquisition card and the Stream Ware software. We estimated the hydraulic characteristic uncertainties for a 95% confidence interval according to the method presented in [34, 35]. The estimated average velocity and temperature uncertainties were equal to ±4% and ±3.6%, respectively. The uncertainty of the measurement of the mean square value of longitudinal velocity and temperature pulsations was estimated as ±8% and ±7%, respectively.

RESULTS AND DISCUSSION

The work studied the average and pulsating dynamic and thermal characteristics of a separate flow with a flow around solitary rectangular ribs with confusor, diffuser, and constant section slits in the turbulent boundary layer that formed upon air flow along the surface of a flat plate heated by the constant heat flux, q_w = const.

Joint measurement of the velocity and temperature distributions and their pulsations in the turbulent boundary layer makes it possible to conduct quantitative and qualitative analyses and to compare the heat transfer in different zones of the boundary layer, including the viscous sublayer.

FLAT PLATE

Figure 2 shows the experimentally determined profiles of the average longitudinal velocities and their pulsations, as well as the average temperatures and their pulsations in three sections on the flat plate before rib placement within this domain. These profiles in the boundary layer in the three sections are typical for a flat wall; the state of the boundary layer corresponds to the completely developed turbulent

Table 1. Sizes of the studied ribs

Variant in Fig. 1	Slit type	Rib height h, mm	Slit size, mm		
			h_1	h_2	b_1
(a)	Confusor	3.2	2.2	0.6	1.5
(b)	Diffuser	3.2	0.6	2.2	1.5
(c)	Constant	3.2	1.0	1.0	3.2

layer. This is indicated by the value of the form parameter in those sections, $H = \delta^*/\delta^{**} = 1.35-1.37$, i.e., it conforms with the one-seventh law.

Pulsations of the velocity and temperature in these three sections (Fig. 2b) are typical for the turbulent boundary layer upon gradient-free flowing around the plate. As in [1, 3, 6, 27], there is a solitary, clearly pronounced maximum at the wall at $(y/\delta) \approx 0.02$. Thus, the zone of the maximal gradient of the velocity and temperature at the wall serves as the source of the turbulence occurrence.

The values of the local friction and heat transfer coefficients presented in Fig. 3 are in good agreement with the well-known laws of friction and heat transfer [1, 25]. The local friction coefficients were determined by the Clauser method according to the logarithmic part of the velocity profile in the boundary layer and the slope of the velocity profile in the laminar sublayer; they are also plotted according to the momentum thickness. The local heat transfer coefficients were calculated according to the energy loss and the
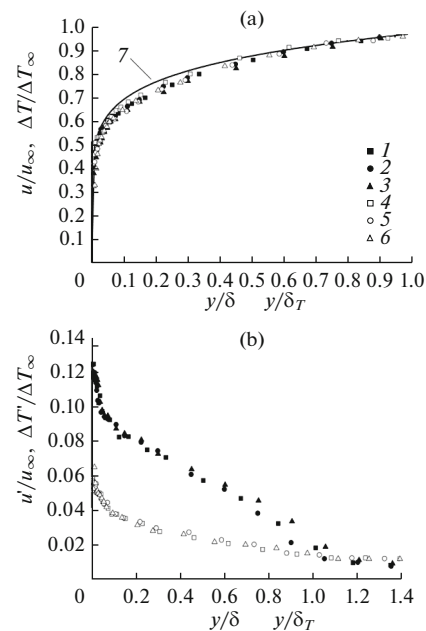

Fig. 2. Distribution of the velocity and temperature (a) and of their pulsations (b) in the boundary layer in three sections (l_x = 450, 500, 550 mm): (*1–3*) velocity, (*4–6*) temperature, (*7*) the one-seventh law.
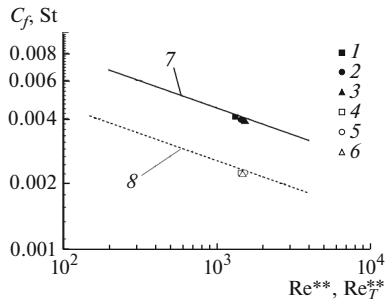
Fig. 3. Friction and heat transfer laws on a flat plate in the three sections (l_x = 450, 500, 550 mm): (*1–3*) C_f, (*4–6*) St, (*7*) $C_f = 0.0252(\text{Re}^{**})^{-0.25}$, (*8*) St $= 0.0144(\text{Re}_T^{**})^{-0.25}$.
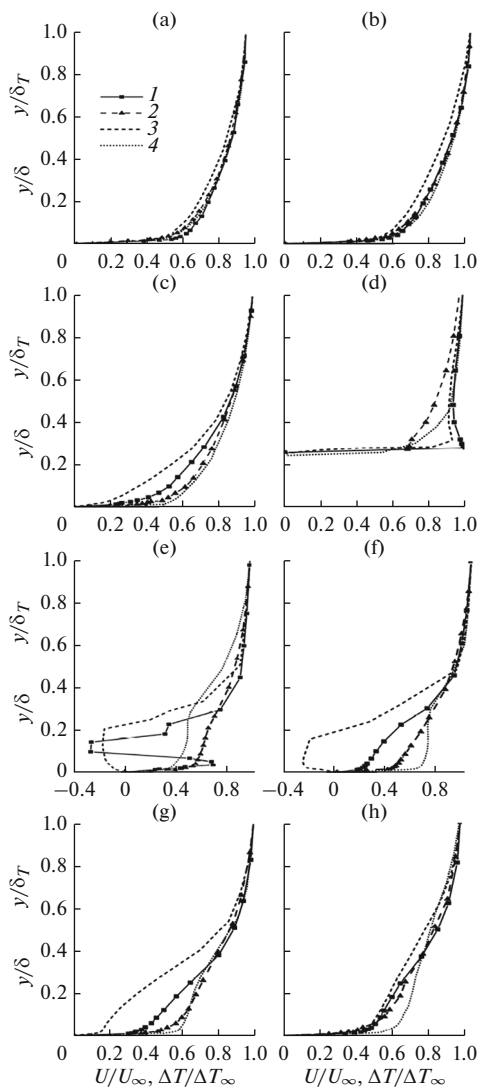

Fig. 4. Velocity and temperature distribution in the boundary layer for a rectangular rib with a confusor slit (*1, 2*) and a solid rib [7] (*3, 4*): (*1, 3*) U/U_∞; (*2, 4*) $\Delta T/\Delta T_\infty$; (a) section 1, $x/h = -11.94$; (b) 2, -5.7; (c) 3, -1.94; (d) 4, -0.5; (e) 5, 0.94; (f) 6, 2.44; (g) 7, 10.25; (h) 8, 18.06.

slope of the temperature profile in the laminar sublayer. This good agreement with the known dependences is evidence of the validity of the used techniques for the determination of the friction and heat-transfer coefficients.

RECTANGULAR RIB WITH CONFUSOR SLIT

The structure of the zero-pressure gradient turbulent boundary layer was studied experimentally, both in front of the rectangular rib and behind it, within the range of the mutual location of the rib and the measurement sections $-11.94 < x/h < 18.06$, where x is the distance from the back rib wall to the studied section and h is the rib height.

Figure 4 shows the velocity and temperature distributions (where $\Delta T = T_w - T$, $\Delta T_\infty = T_w - T_\infty$) in the boundary layer in the eight sections belonging to the range indicated above, for a rectangular rib with a confusor slit (Fig. 1a). The results show that, in the approach to the rib (the first, $x/h = -11.94$, and the second, $x/h = -5.7$, sections), the velocity and temperature profiles remain constant; however, upon the further approach to the rib, beginning from the third section, $x/h = -1.94$, the velocity profile deforms and becomes less full. The increase in the form parameter, $H = 1.37$, 1.41, and 1.62, also confirms this fact. Unlike the velocity profile, the temperature profiles react weakly to the rib and in fact coincide with the one-seventh law. They are fuller than those of the velocity (corresponding to the data in [7]), i.e., they react more conservatively to the rib effect and the variation in its shape.

In the vicinity of section 3 ($x/h = -1.94$), unlike the results [7] for the solid rectangular rib, no vortex or stagnant zone was observed (see the profiles of the longitudinal velocity and its pulsations, Figs. 4 and 5). The flow character in front of the slit rib differs drastically from that in front of the solid rib [7]. In the case of the confusor rib, part of the near-wall flow rushes to the slit and accelerates; another part bends round the rib and rushes to the wall behind it.

Figure 5 shows the distributions of the velocity and temperature pulsations in the boundary layer for a rectangular rib with a confusor slit. In front of the rib, in all sections, the distributions of the velocity and temperature pulsations in fact coincide with the respective characteristics for the gradient-free flow around a plate without a rib. In section 3, the maximum of the velocity pulsation at the wall somewhat increases at the slit entrance. This is most likely related to the flow acceleration at the entrance to the profiled slit.

In section 4, the velocity and temperature pulsation somewhat increase above the rib. Note that the character of the studied parameter variations depends significantly on the location of the measurement section above the rib.

Behind the rib, a complicated flow occurs (Figs. 4 and 5). Within the domain between the sections 5 and 8 ($0.94 < x/h < 18.06$), there is a mixture of the external flow, which separates from the rib surface, and the accelerated near-wall flow, which flows from the confusor slit. There is strong deformation of the temperature profiles, especially of the profiles of the velocity and its pulsations. The increase in the form parameter in sections 6–7, $H = 4.31$ and 2.19, indicates the significant influence of the rib on the velocity profiles. The temperature profiles behind the rib and their pulsations vary slightly. There is a minor bound vortex directly behind the rib (section 5, $x/h = 0.94$) in its upper part ($h - h_2$), unlike the flow around the solid rib [7] (see the profile of the velocity and its pulsations, Figs. 4 and 5). The reverse of the flow velocity direction (Fig. 4e) also indicates the occurrence of a bound vortex. In section 6 ($x/h = 2.44$), we did not see any traces of the vortex; in sections 7 and 8, the boundary layer returns to its normal state, which corresponds to the gradient-free turbulent flow around the plate.

In the present experimental studies of flow around a rib with a confusor slit, we did not observe separation zones in front of the rib or behind it. However, significant variations in the velocity profile and its pulsation take place directly behind the backward-facing step (Figs. 4e and 5e). There are three maxima in the velocity pulsation distribution (Fig. 5e) and two in the temperature pulsation distribution. Thus, three sources of the turbulence occurrence exist in the velocity pulsation distribution behind the rib: the heat-transfer surface, the confusor surface of the rib, and the zone of the main flow separation from the upper rib surface. In section 5, the velocity pulsations at the wall somewhat exceed the intensity of the turbulence in the mixture zone. Moreover, the maximum of the velocity pulsations significantly exceeds that of the temperature pulsations in the mixture zone above the rib (Fig. 5), since the velocity profile is more deformed than the temperature profile. The temperature pulsations have two minor maxima: at the wall and in the mixture zone. Already in section 6, the second maximum of the velocity pulsations merges with the first; beginning from that section, both the temperature pulsations and the velocity pulsations have only two maxima. Then, in the mixture zone, the velocity pulsation maximum grows sufficiently faster than the wall maximum and surpasses it.

Considering the velocity and the temperature profiles (Fig. 4), we see that they have certain breaks. The first breaks in the velocity and temperature profiles coincide with the maxima of the respective pulsations with an initially smooth surface, the heat-transfer surface; the second breaks coincide with the second maximum of the respective pulsations located within the zone of flow separation from the external rib surface. Then, we see that the reverse flow is absent behind the rib with the confusor slit. Note that, for the solid rib,
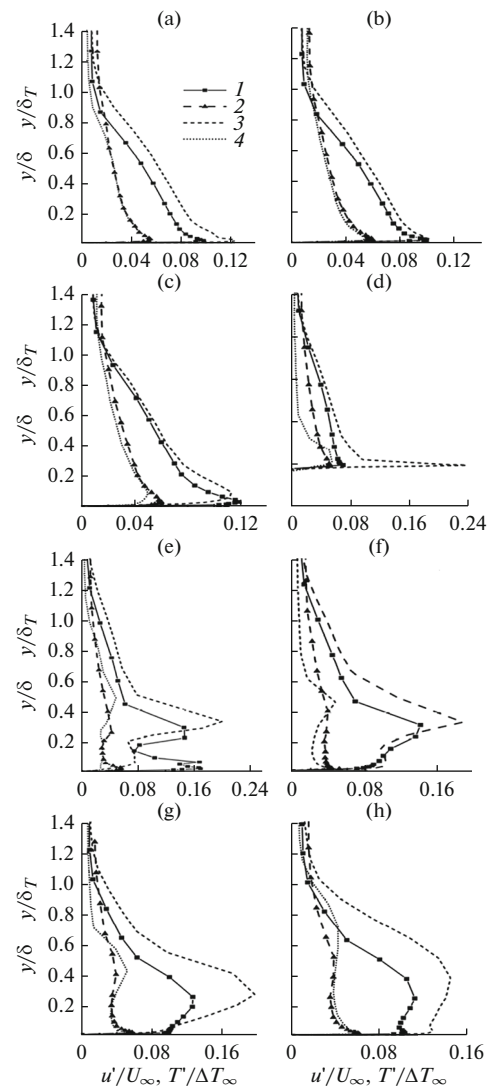

Fig. 5. Distribution of velocity and temperature pulsations in the boundary layer for a rectangular rib with a confusor slit (*1, 2*) and a solid rib [7] (*3, 4*): (*1, 3*) u'/U_∞; (*2, 4*) $T'/\Delta T_\infty$; (a)–(h) the same as in Fig. 4.
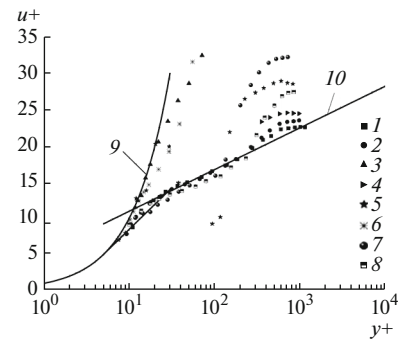

Fig. 6. Universal logarithmic law of the velocity distribution with flow around a rectangular rib with a confusor slit: $x/h = -11.94$ (*1*), -5.7 (*2*), -1.94 (*3*), -0.5 (*4*), 0.94 (*5*), 2.44 (*6*), 10.25 (*7*), 18.06 (*8*); (*9*) calculation according to (1), (*10*) to (2).
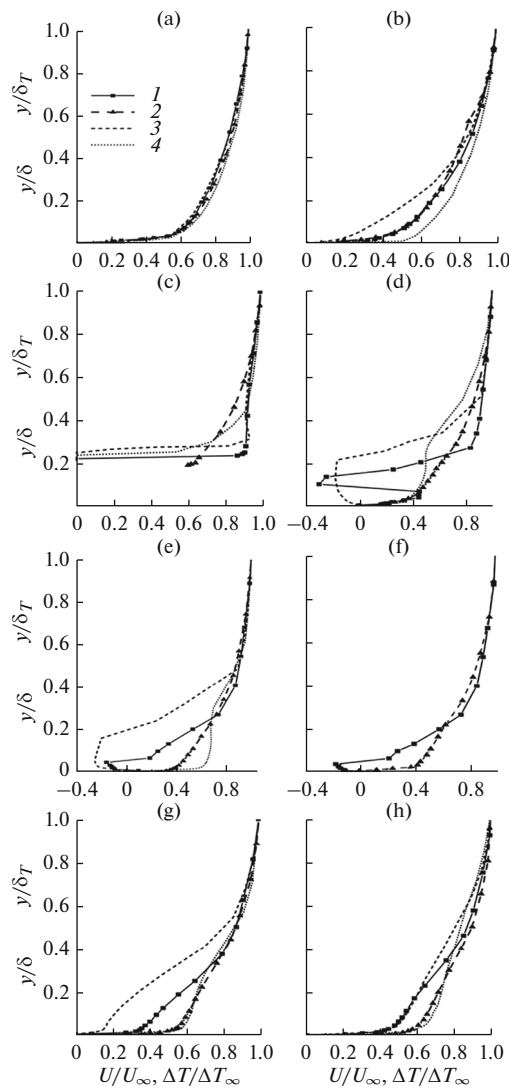
Fig. 7. Velocity and temperature distribution in the boundary layer for a rectangular rib with a diffuser slit (*1, 2*) and a solid rib [7] (*3, 4*): (*1, 3*) U/U_∞; (*2, 4*) $\Delta T/\Delta T_\infty$; (a) section 1, $x/h = -12.6$; (b) 2, -2; (c) 3, 0; (d) 4, 1; (e) 5, 2; (f) 6, 3; (g) 7, 10; (h) 8, 18.13.

Figure 6 shows a comparison of the experimentally obtained velocity profiles with the universal logarithmic law of the velocity distribution over the turbulent boundary layer on a flat plane:

$$u^+ = y^+ \text{ for } y^+ < 5, \qquad (1)$$

$$u^+ = 5.75\log y^+ + 5.2 \text{ for } y^+ > 30, \qquad (2)$$

where $u^+ = u/u_\tau$ is the dimensionless velocity; $y^+ = yu_\tau/\nu$ is the dimensionless coordinate; and $u_\tau = (\tau_w/\rho)^{0.5}$ is the dynamic velocity.

Such a presentation of the velocity profiles makes it possible to discuss the state of the boundary layer in the given section. If the universal law describes the obtained velocity distributions rather exactly, then the flow in the boundary layer is turbulent and gradient-free. Thus, with Fig. 6, we might discuss the degree of impact of the turbulizer (the rib) on the wall domain of the boundary layer, primarily on the laminar sublayer, the buffer domain, and the logarithmic part of the boundary layer. The dynamic rate at which the logarithmic profiles were processed was determined according to the logarithmic part of the velocity profile in the boundary layer (the Clauser method) and to the slope of the velocity profile in the laminar sublayer (Newton's law) in sections 1, 2, and 8. In the separation zones, where there is no logarithmic domain in the velocity profiles, the dynamic velocity was calculated only by the slope of the velocity profile in the laminar sublayer (Newton's law). Figure 6 shows that the velocity profile in sections 1 and 2 does not in fact react to the rib approach; the standard turbulent boundary layer occurs there. After the rib, in profiles 7 and 8, the standard turbulent boundary layer is also restored. The profiles of the average velocities and temperatures behind the rib between the sixth and the seventh sections are formed after the flow separated from the rib surface mixes with the wall jet emanating from the slit. As the result, a new boundary layer occurs and gradually returns to the one-seventh law (Fig. 6).

RECTANGULAR RIB WITH A DIFFUSER SLIT

Figure 7 shows the measured velocity and temperature profiles in the boundary layer for a rectangular rib with a diffuser slit (Fig. 1b) in the interval $-12.6 < x/h < 18.13$. Given the results presented in Figs. 7 and 8, we see that the profiles of the velocity, temperature, and their pulsations behind the rib coincide with similar results for a rib with a confusor slit.

For the diffuser slit, as for the confusor slit, part of the near-wall flow rushes into the slit; there, the flow decelerates in the expanding part of the slit. At the exit, behind the rib, this flow part interacts with the flow part that flows around the rib and, separating from it, rushes to the wall. The flow pattern behind the rib with a diffuser slit is in general similar to that of the flow

the domain of its existence is about $x/h = 7-8$ calibers [7].

The velocity pulsations behave differently; from their distribution, we see (Fig. 5) that the velocity pulsation maximum remains at the streamline originating at the upper vortex boundary and that the domain of more intensive pulsations widens, i.e., the turbulent pulsations occurring at the upper vortex boundary are transferred by the averaged flow along the streamlines, which gradually decay and diffuse away from it. Thus, when the rib moves away, the pulsation maximum zone widens and increases; however, it does not influence the average characteristics. The profiles of the average velocities and the average temperatures behind the rib return to the one-seventh law.

around a solid rectangular rib [7]. However, the separation zone behind the slit rib turns out to be significantly wider ($x/h \approx 4-5$) than the similar zone ($x/h \approx 8$) for a solid rectangular rib [7].

The distribution of the velocity pulsation in the last sections ($x/h = 5-18.13$) illustrates the difference in the rib influence on the pulsation characteristics of the boundary layer. In the considered sections, the profiles of the averaged velocities and temperatures approach the one-seventh law, whereas the velocity and temperature pulsations there are significantly higher than the same for the corresponding parameters with a gradient-free flow.

Directly behind the backward-facing step, in the section $x/h = 1$ (Fig. 8), there are pronounced changes in the velocity and temperature pulsations. In the velocity and the temperature pulsation distribution, there are two maxima, i.e., there are two sources of turbulence origin for the velocity pulsations: the heat-transfer surface and the zone of the main flow separation from the upper rib surface. In all sections behind the rib, the velocity pulsations in the mixture zone are significantly higher than those at the wall. Moreover, behind the rib in the mixture zone (Fig. 8), the velocity-pulsation maximum significantly exceeds that of the temperature pulsations. The same pattern also occurs in the case of the rib with a confusor slit (Fig. 5). There are two maxima for the temperature pulsations: at the wall and in the mixture zone. The velocity-pulsation maximum in the mixture zone increases much faster than the wall maximum and surpasses it. With flow development behind the rib, the pulsation maximum somewhat decreases; however, the pulsation profile becomes fuller and thicker. As with the confusor slit, the velocity pulsations differ significantly from the gradient-free flow.

The distribution of the average velocities in the universal logarithmic coordinates coincides in many respects with that for the rib with a confusor slit.

RECTANGULAR RIB WITH A CONSTANT CROSS-SECTION SLIT

The velocity and the temperature profiles and their pulsations were measured in eight sections of the boundary layer for a rectangular rib with a constant cross-section slit (Fig. 1c) in the interval $-11.94 < x/h < 20.88$.

The results (Figs. 9 and 10) show that the velocity and the temperature profiles and their pulsations in front of the rib coincide, in fact, with similar results for ribs with confusor and diffuser slits. In the vicinity of section 3 (in front of the rib, $x/h = -1.94$), as in these cases (unlike the results [7] for a solid rectangular rib), we do not observe a vortex in front of the slit rib; it follows from the velocity profiles and their pulsations (Figs. 9 and 10).
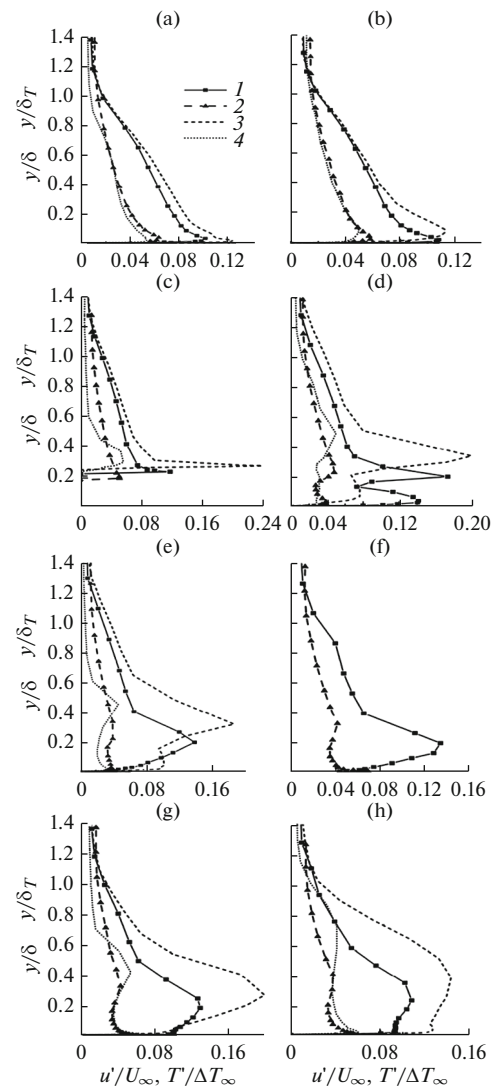

Fig. 8. Distribution of velocity and temperature pulsations in the boundary layer for a rectangular rib with a diffuser slit (*1, 2*) and a solid rib [7] (*3, 4*): (*1, 3*) u'/U_∞; (*2, 4*) $T'/\Delta T_\infty$; (a)−(h) the same as in Fig. 7.

As in the aforementioned cases of ribs with confusor and diffuser slits, part of the near-wall flow rushes into the slit and accelerates. At the exit behind the rib, this part of the flow interacts with the flow part that flows around the rib and, separating from it, rushes to the wall. Behind the rib with a constant cross-section slit, the flow pattern is similar in many respects to that for the confusor slit. However, in the considered case, a minor domain of reversed flow occurs in the upper rib part (in the section $x/h = 0.56$ in Figs. 9 and 10). In the section $x/h = 2.13$, there is a very thin separation zone.

Figure 10 shows the distribution of the velocity and temperature pulsations in the boundary layer for a rectangular rib with a constant cross-section slit. In all of the sections in front of the rib, they coincide with
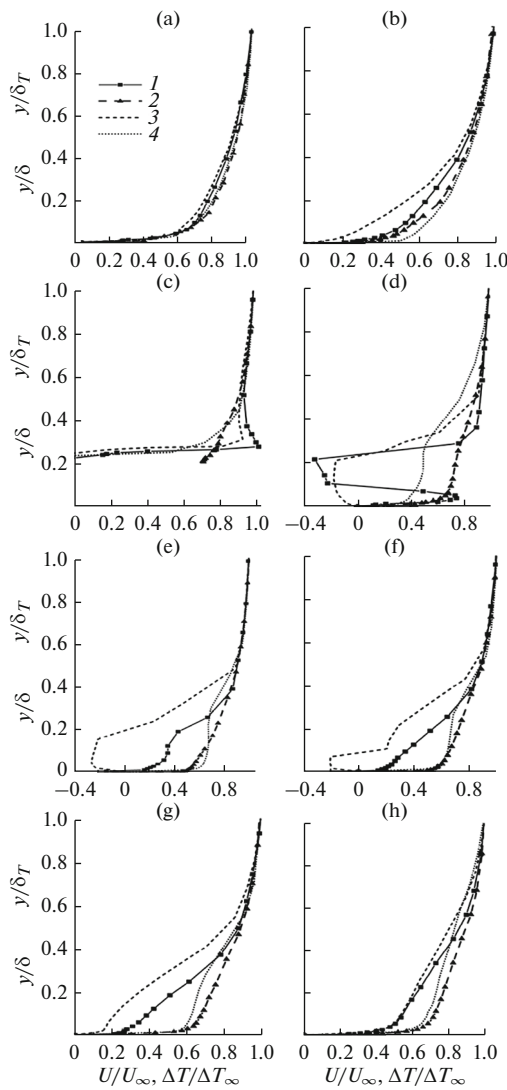
Fig. 9. Velocity and temperature distribution in the boundary layer for a rectangular rib with a constant cross-section slit (1, 2) and a solid rib [7] (3, 4): 1, $3 - U/U_\infty$; 2, $4 - \Delta T/\Delta T_\infty$; (a) − section 1, $x/h = -11.94$; (b) 2, -1.94; (c) 3, -0.5; (d) 4, 0.56; (e) 5, 2.13; (f) 6, 5.25; (g) 7, 8.38; (h) 8, 20.88.
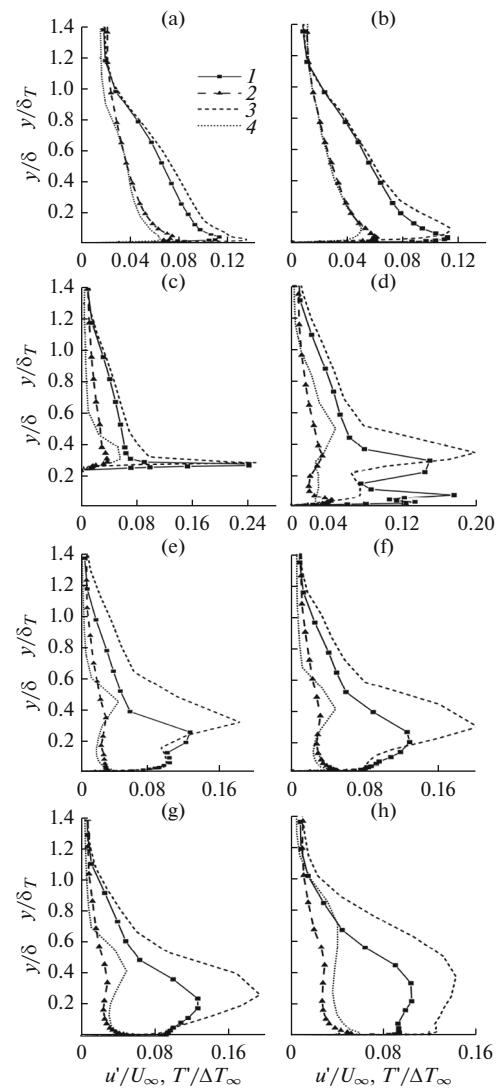
Fig. 10. Distribution of velocity and temperature pulsations in the boundary layer for a rectangular rib with a constant cross-section slit (1, 2) and a solid rib [7] (3, 4): (1, 3) u'/U_∞; (2, 4) $T'/\Delta T_\infty$; (a)−(h) the same as in Fig. 9.

the corresponding characteristics of the gradient-free flow around the plate.

Behind the considered slit rib, there is a complicated vortex flow similar to that occurring with flow around the rib with a confusor slit. Here, the temperature profile does not vary. In the separation zone, the velocity and temperature pulsations vary significantly (Fig. 10). Here, we see three maxima in the distribution of the velocity pulsations and two maxima in the distribution of the temperature pulsations (Fig. 10, section 5), as in the case of flow around the rib with a confusor slit.

The distribution of the average velocities in the universal logarithmic coordinates is similar in many

respects to the cases of ribs with confusor and diffuser slits.

CONCLUSIONS

The hydrodynamics and heat transfer processes in a turbulent air flow around the surface of a plate heated by a constant heat flux, q_w = const, with rectangular ribs ($\delta/h \approx 4$) with confusor, diffuser, and constant cross-section slits across the flow were studied experimentally. Experimental data was obtained based on the average and pulsation characteristics of the velocity and the temperature along the plate middle at sections of the turbulent boundary layer with a flow around slit rectangular ribs. It was shown that the vor-

tex and separation zones do not occur in front of the slit rib. In the boundary layer behind the slit ribs, the temperature pulsations have two maxima; the velocity pulsations for the confusor and the constant cross-section slits are characterized by three maxim, and these maxima are significantly higher than those in the gradient-free flow over a flat wall. In the case of a diffuser slit, the temperature and velocity pulsations have two maxima in the boundary layer, and these maxima are significantly higher than those in the flow over a flat wall. It was found that there is no recirculation zone behind the rib with the confusor slit, whereas it is significantly shorter ($x/h < 2.5$ and 5 m, respectively) behind a rib with a constant cross-section and a diffuser slit than behind a solid rib ($x/h \approx 8$).

FUNDING

REFERENCES

1. Afanas'ev, V.N., Veselkin, V.Yu., Leont'ev, A.I., Skibin, A.P., and Chudnovskii, Ya.P., Hydrodynamics and heat transfer in a flow around a single depression on an initially smooth surface, *Preprint of Bauman Moscow State Tech. Univ.,* Moscow, 1991, no. 2−91.

2. Burtsev, S.A., Kiselev, N.A., and Leont'ev, A.I., *High Temp.*, 2014, vol. 52, no. 6, p. 895.

3. Afanasyev, V.N., Chudnovsky, Ya.P., Leontiev, A.I., and Roganov, P.S., *Exp. Therm. Fluid Sci.*, 1993, vol. 7, p. 1.

4. Leontiev, A.I., Kiselev, N.A., Burtsev, S.A., Strongin, M.M., and Vinogradov, Y.A., *Exp. Therm. Fluid Sci.*, 2016, vol. 79, p. 74.

5. Afanas'ev, V.N. and Kon Dehai, *Nauka Obraz.*, 2017, no. 4.
   https://doi.org/10.7463/0417.0000932

6. Afanasiev, V.N. and Kong Dehai, *J. Phys.: Conf. Ser.*, 2017, vol. 891, 012140.

7. Afanasiev, V.N., Trifonov, V.L., Getya, S.I., and Kong Dehai, *Mashinostr. Kompyut. Technol.*, 2017, no. 10. http://www.technomagelpub.ru/jour/article/view/1312.

8. Fouladi, F., Henshaw, P., Ting, D.S.-K., and Ray, S., *Int. J. Heat Mass Transfer*, 2017, vol. 104, p. 1202.

9. Larichkin, V.V. and Yakovenko, S.N., *J. Appl. Mech. Tech. Phys.*, 2003, vol. 44, no. 3, p. 365.

10. Kalinin, E.K., Dreitser, G.A., and Yarkho, S.A., *Intensifikatsiya teploobmena v kanalakh* (Intensification of Heat Transfer in the Channels), Moscow: Mashinostroenie, 1990.

11. *Teploobmen v dozvukovykh otryvnykh potokakh* (Heat Transfer in Subsonic Tearing Streams), Terekhov, V.I., Ed., Novosibirsk: Novosibirsk. Gos. Tekh. Univ., 2016.

12. Terekhov, V.I., Yarygina, N.I., and Zhdanov, R.F., *Int. J. Heat Mass Transfer*, 2003, vol. 46, p. 4535.

13. Smulsky, Ya.I., Terekhov, V.I., and Yarygina, N.I., *Int. J. Heat Mass Transfer*, 2012, vol. 55, p. 726.

14. Wang, L. and Sunden, B., *Heat Mass Transfer*, 2007, vol. 43, p. 759.

15. Ligrani, P., *Int. J. Rotating Mach.*, 2013, vol. 2013, no. 275653, p. 32.

16. Ji, W.T., Jacobi, A.M., He, Y.L., and Tao, W.Q., *Int. J. Heat Mass Transfer*, 2015, vol. 88, p. 735.

17. Molochnikov, V.M., Mikheev, N.I., Davletshin, I.A., and Paerelii, A.A., *Izv. Ross. Akad. Nauk, Energ.* 2008, no. 1, p. 137.

18. Nagano, Y., Hattori, H., and Houra, T., *Int. J. Heat Fluid Flow*, 2004, vol. 25, p. 393.

19. Wang, L., Salewski, M., and Sunden, B., *Exp. Therm. Fluid Sci.*, 2010, vol. 34, p. 165.

20. Panigrahi, P.K., Schröder, A., and Kompenhan, J., *Exp. Fluids*, 2006, vol. 40, p. 277.

21. Huang, J.J. and Liou, T.M., *J. Turbomach.*, 1997, vol. 119, p. 617.

22. Huang, J.J. and Liou, T.M., *J. Heat Transfer*, 1994, vol. 116, p. 912.

23. Tariq, A., Panigrahi, P.K., and Muralidhar, K., *Exp. Fluids*, 2004, vol. 37, p. 701.

24. Liou, T.M., Yang, C.P., and Lee, H.L., *J. Heat Transfer*, 1997, vol. 119, p. 383.

25. Tisa, J.P. and Huang, J.J., *Int. J. Heat Mass Transfer*, 1999, vol. 42, p. 2071.

26. Liou, T.M. and Chen, S.H., *Int. J. Heat Mass Transfer*, 1998, vol. 41, p. 1795.

27. Ahn, J. and Lee, J.S., *Int. J. Heat Mass Transfer*, 2010, vol. 53, p. 445.

28. Terekhov, V.I. and Bogatko, T.V., *Tepl. Protsessy Tekh.*, 2015, vol. 7, no. 2, p. 57.

29. Liu, H.C. and Wang, J.H., *Int. J. Heat Mass Transfer*, 2011, vol. 54, p. 575.

30. Migai, V.K., *Povyshenie effektivnosti teploobmennikov* (Improving the Efficiency of Heat Exchangers), Leningrad: Energiya, 1980.

31. Belov, I.A., Isaev, S.A., and Korobkov, V.A., *Zadachi i metody rascheta otryvnykh techenii neszhimaemoi zhidkosti* (Problems and Methods for Calculating Separated Flows of Incompressible Fluid), Leningrad: Sudostroenie, 1989.

32. Isaev, S.A., Vatin, N.I., Guvernyuk, S.V., Gagarin, V.G., Basok, B.I., and Zhukova, Yu.V., *High Temp.*, 2015, vol. 53, no. 6, p. 873.

33. Afanas'ev, V.N. and Trifonov, V.L., *Intensifikatsiya teplootdachi pri vynuzhdennoi konvektsii* (Intensification of Heat Ttransfer during Forced Convection), Moscow: Mosk. Gos. Tekh. Univ. im. N. E. Baumana, 2007.

34. Jorgensen, F.E., *How to Measure Tturbulence with Hot-Wire Anemometers: A Practical Guide*, Skovlunde: Dantec Dynamics, 2002.

35. Moffat, R.J., *Exp. Therm. Fluid Sci.*, 1988, vol. 1, p. 3.

Translated by I. Dikhter